Electronic Supplementary Material (ESI) for Dalton Transactions.

Interfacial synthesized Fe-soc-MOF nanoparticles combined with ICG for photothermal/photodynamic therapy

Xuechao Cai,[ab,‡] Bei Liu,[ab,‡] Maolin Pang[*a] and Jun Lin[*a]

a. State Key Laboratory of Rare Earth Resource Utilization, Changchun Institute of Applied Chemistry, Chinese Academy of Sciences, Changchun 130022, PR China

b. University of the Chinese Academy of Sciences, Beijing 100049, PR China

‡ These authors contributed equally to this work.

* Corresponding author. E-mail address: mlpang@ciac.ac.cn, jlin@ciac.ac.cn

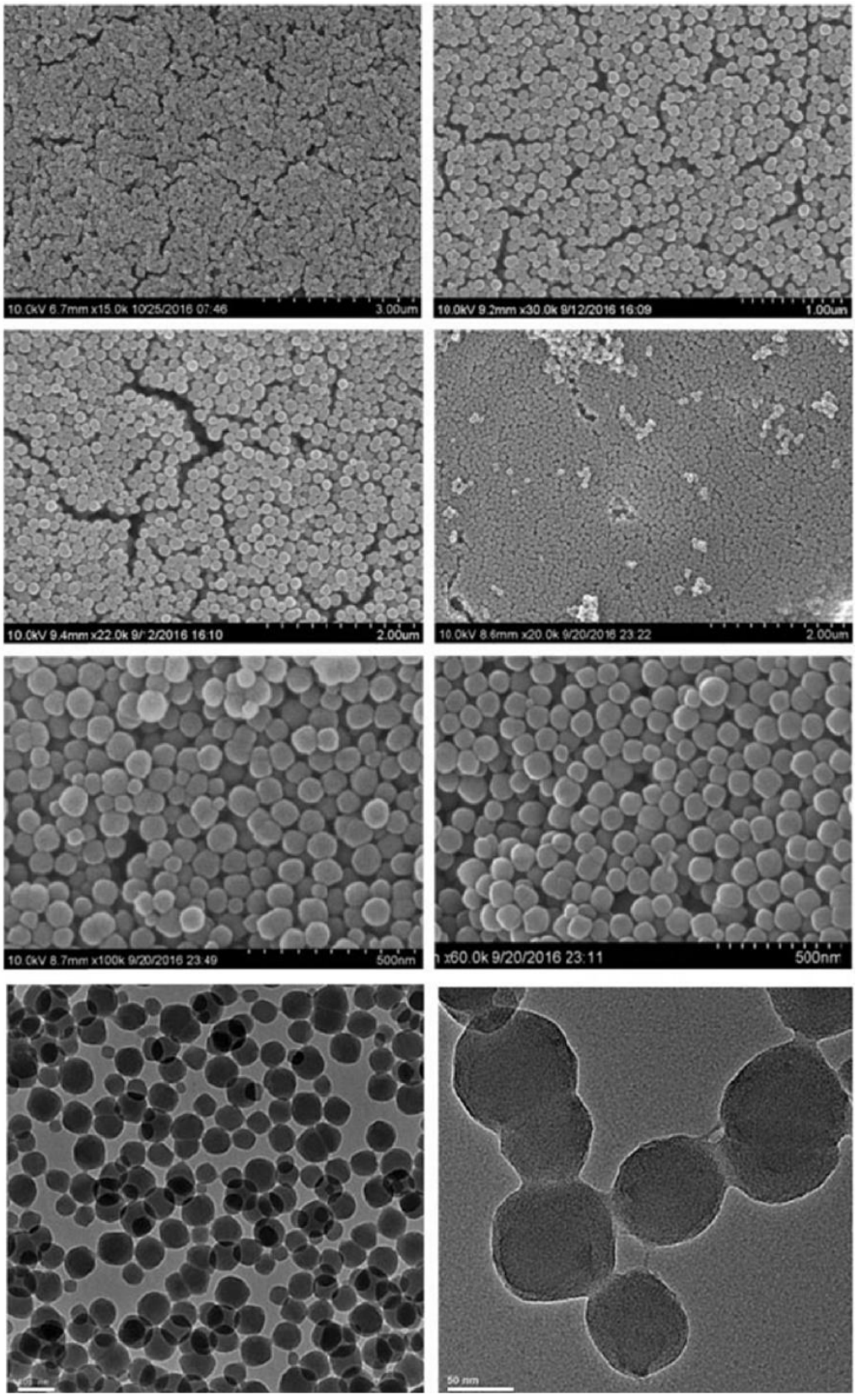

Fig. S1 Additional SEM and TEM images of Fe-**soc**-MOF nanoparticles.

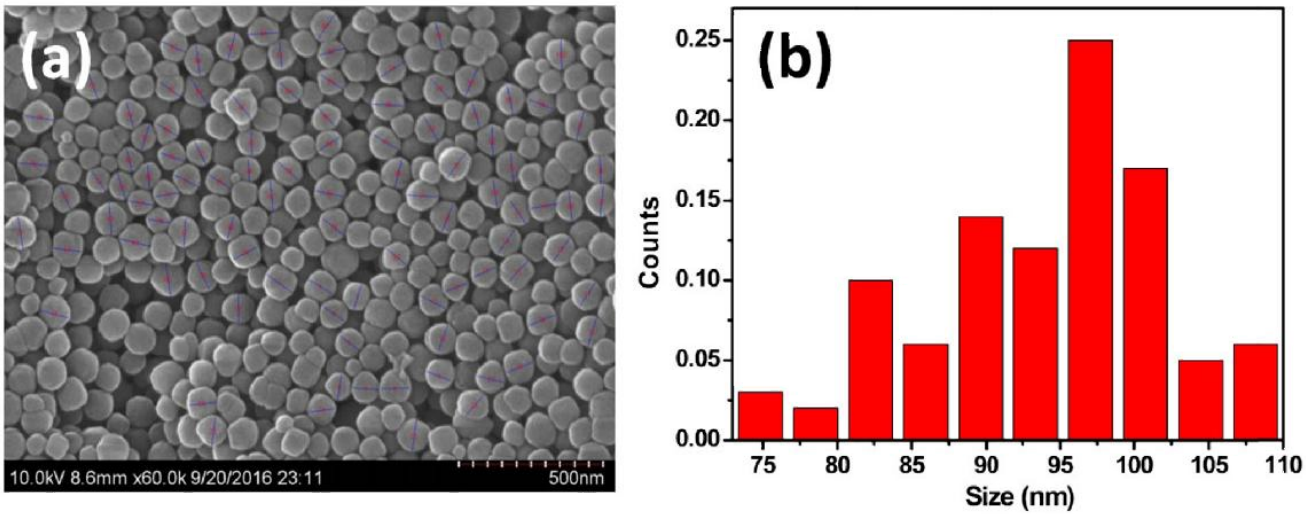

Fig. S2 (a) SEM images of Fe-**soc**-MOF nanoparticles dispersed in ethanol, (b) particle size distribution obtained by counting about 100 particles.

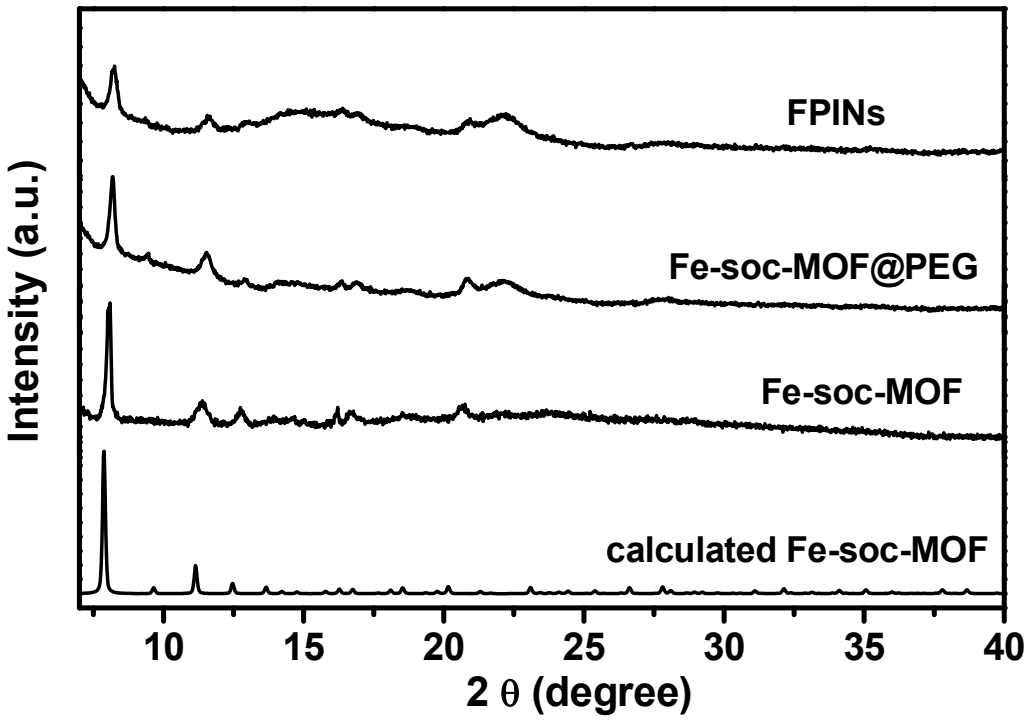

Fig. S3 PXRD patterns of Fe-**soc**-MOF, Fe-**soc**-MOF@PEG and FPINs.

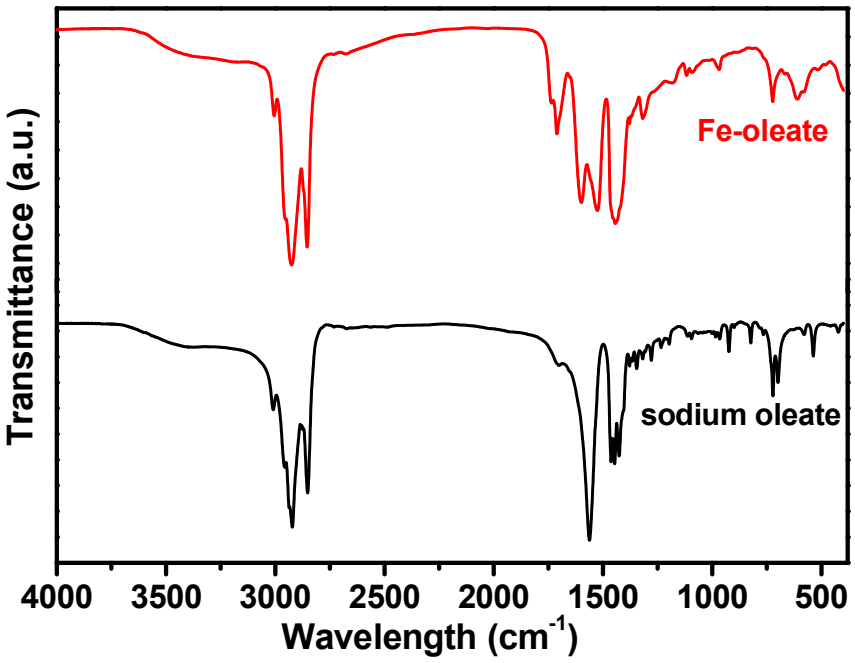

Fig. S4 FT-IR spectra of iron-oleate complex and sodium oleate.

Fig. S5 Photos taken at different reaction times for Fe-**soc**-MOF.

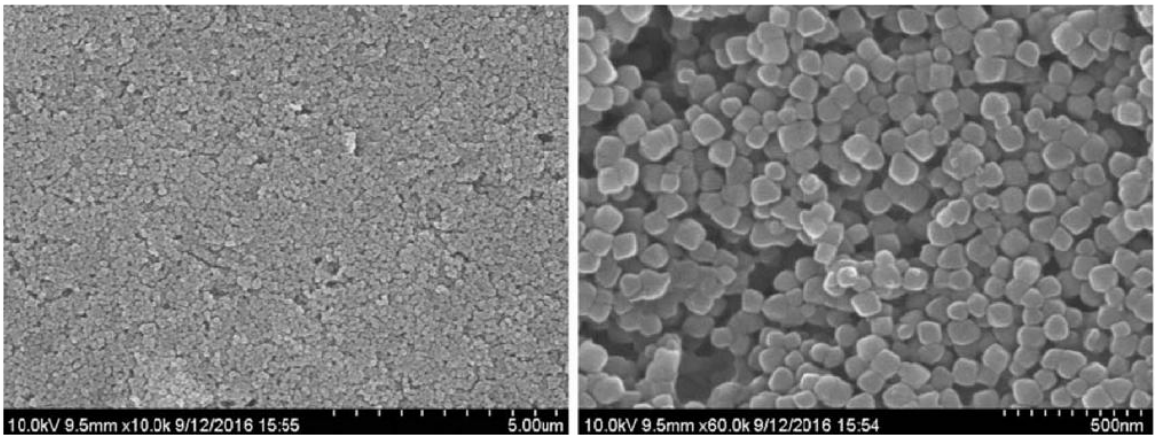

Fig. S6 SEM images of Fe-**soc**-MOF nanoparticles prepared in the absence of triethylamine.

.

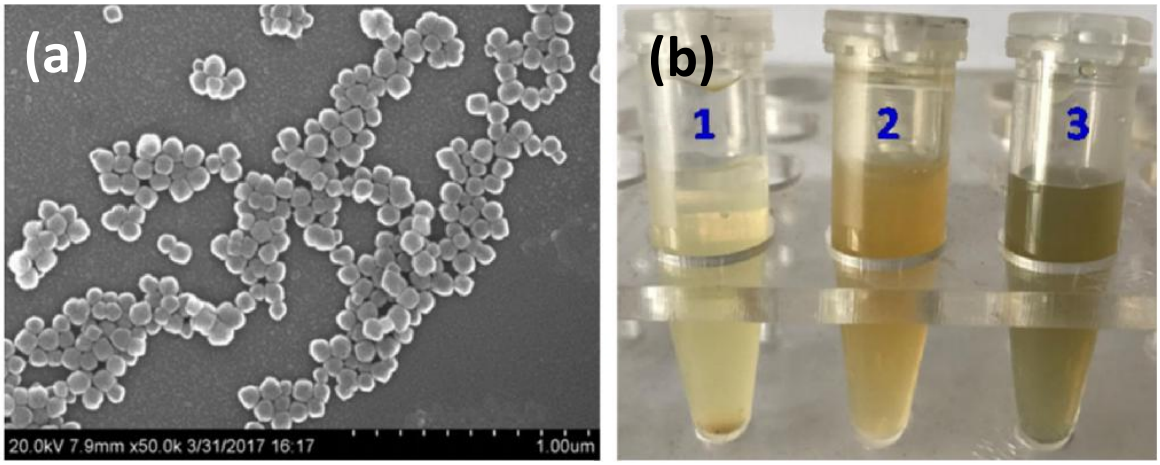

Fig. S7 (a) SEM images of Fe-**soc**-MOF@PEG nanoparticles dispersed in water. (b) Photographs of Fe-**soc**-MOF, Fe-**soc**-MOF@PEG and FPINs after dispersed in water for 6h.

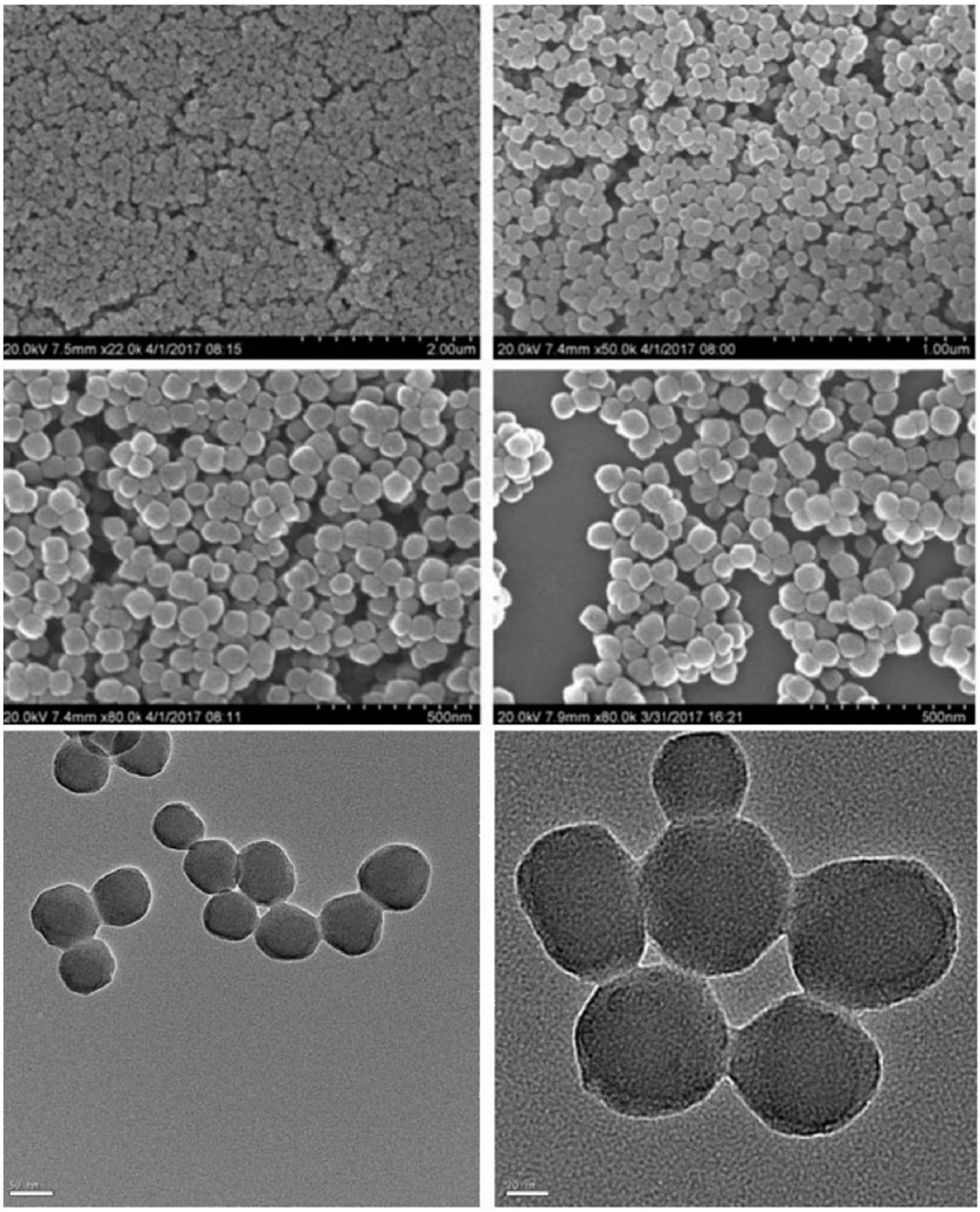

Fig. S8 SEM and TEM images of FPINs.

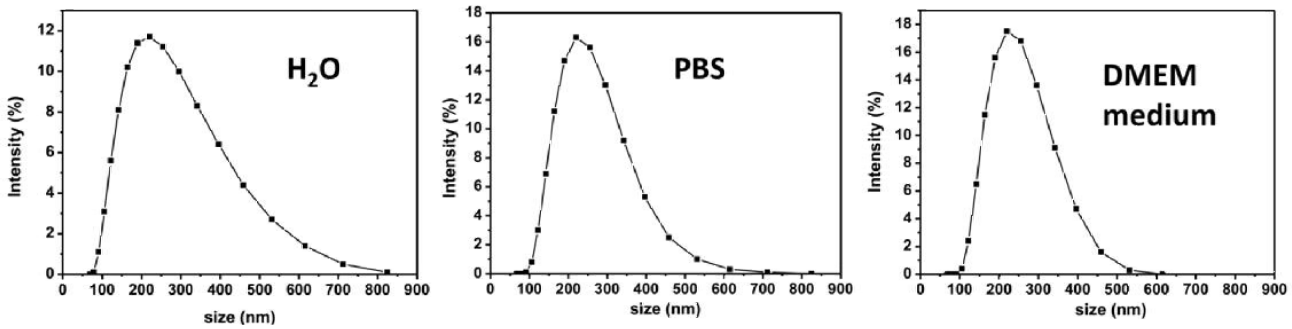

Fig. S9 DLS results for FPINs suspended in H_2O, PBS (pH = 7.4) and DMEM culture medium containing 10% of fetal bovine serum, respectively.

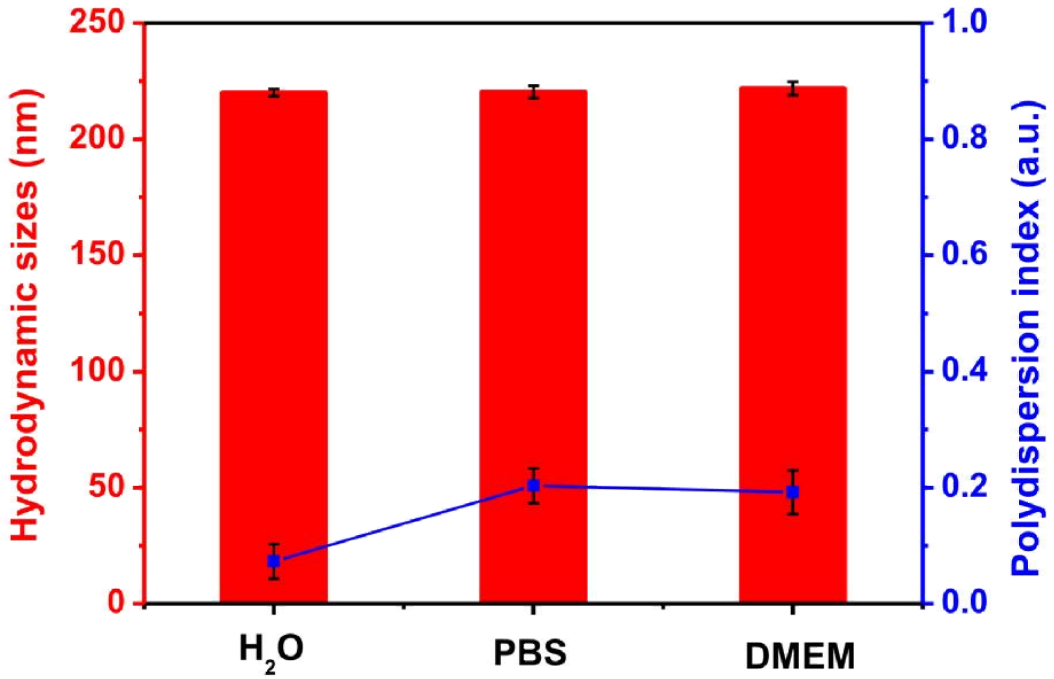

Fig. S10 The average hydrodynamic size and the corresponding polydispersity index of FPINs suspended in H_2O, PBS (pH = 7.4) and DMEM culture medium containing 10% of fetal bovine serum, respectively.

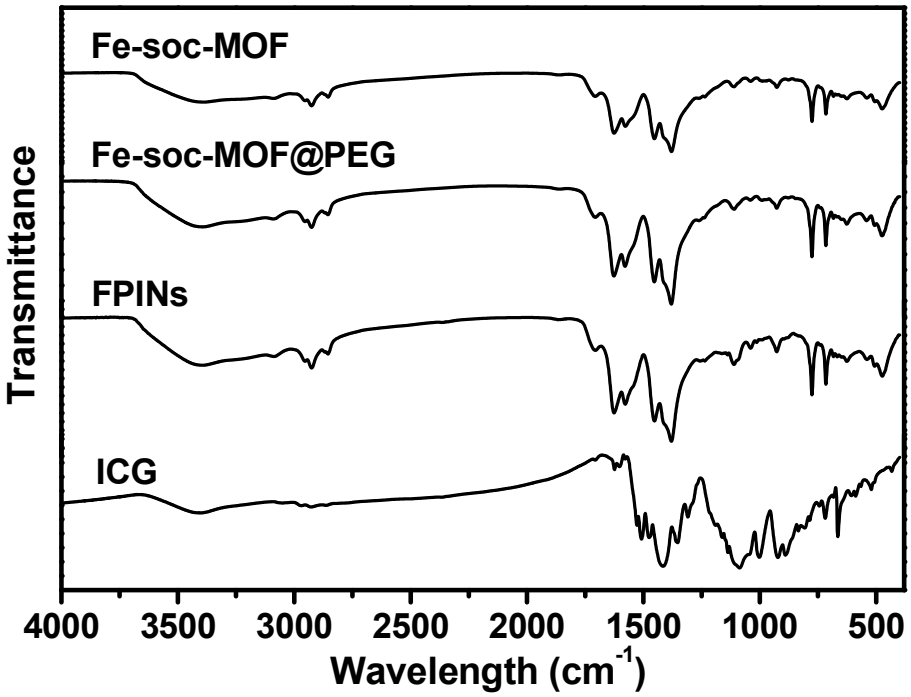

Fig. S11 FT-IR spectra of Fe-**soc**-MOF, Fe-**soc**-MOF@PEG, FPINs and pure ICG.

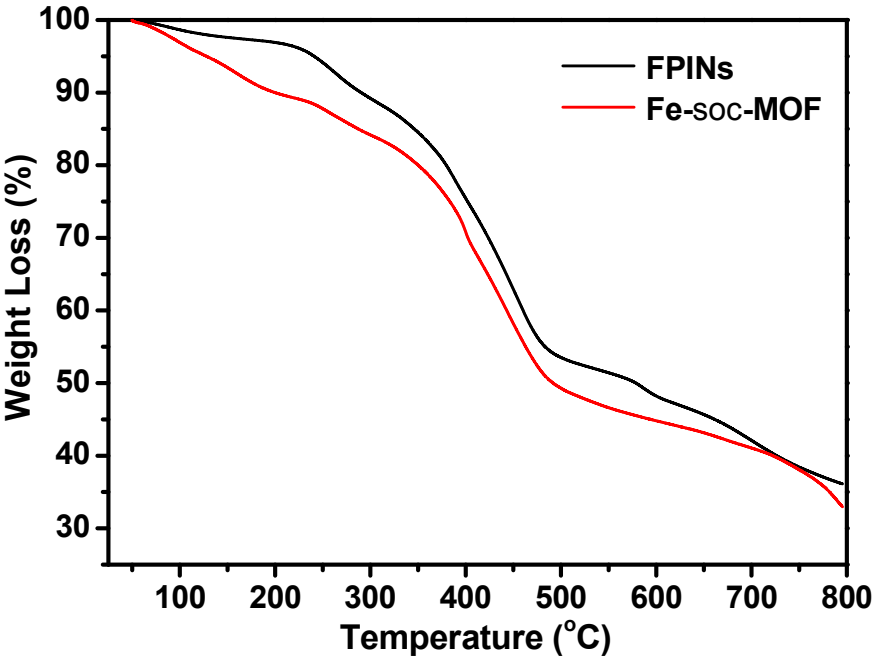

Fig. S12 TGA curves for Fe-**soc**-MOF and FPINs.

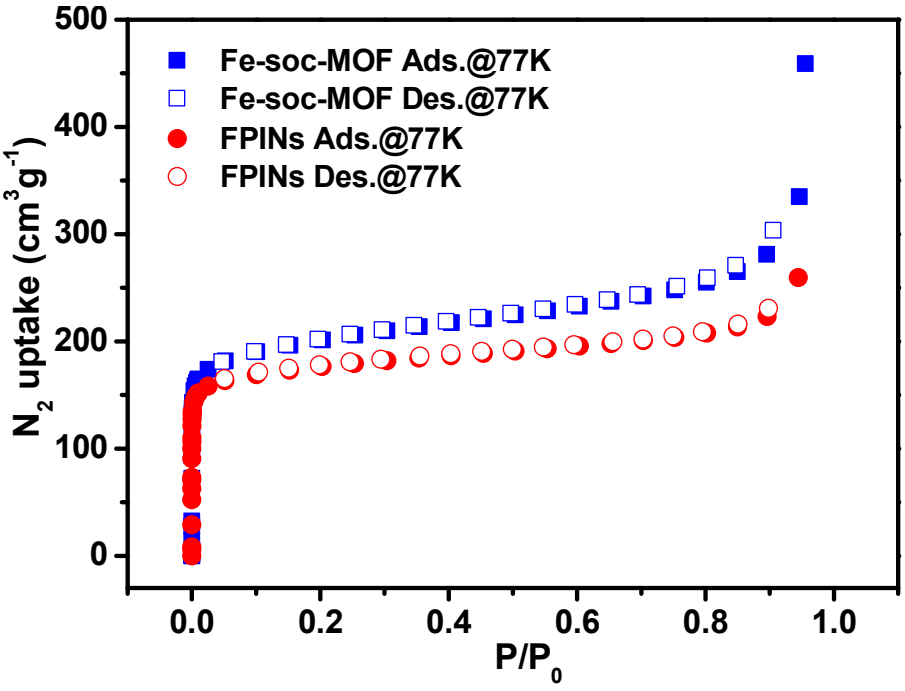

Fig. S13 N_2 adsorption-desorption isotherms for Fe-**soc**-MOF and FPINs.

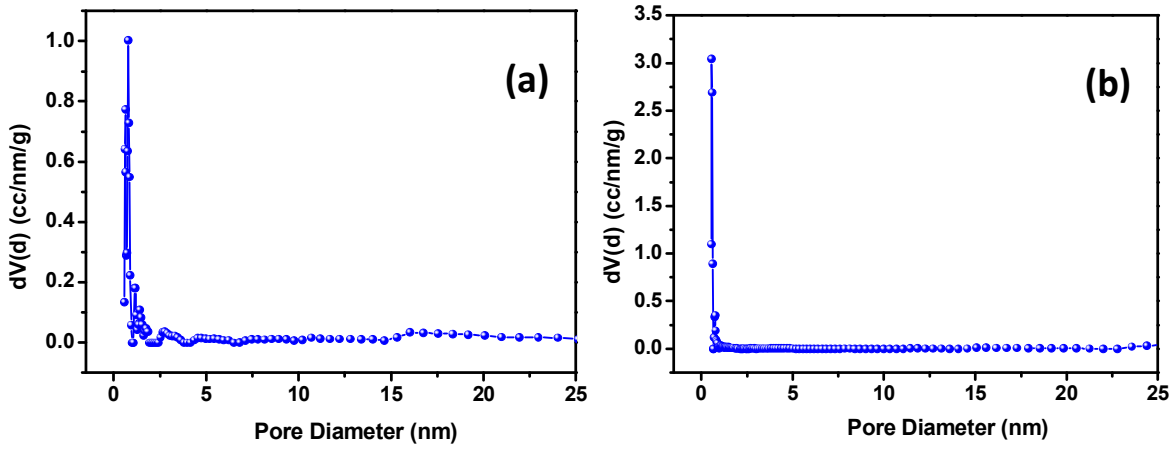

Fig. S14 Pore size distribution curves for (a) Fe-**soc**-MOF and (b) FPINs.

Table S1. Sorption data summary for Fe-**soc**-MOF and FPINs.

Property	Fe-soc-MOF	FPINs
BET surface area ($m^2 g^{-1}$)	757.45	678.46
Langmuir surface area ($m^2 g^{-1}$)	944.74	902.58
Pore volume ($cm^3 g^{-1}$)	0.395	0.315
Pore width (nm)	0.67	0.57

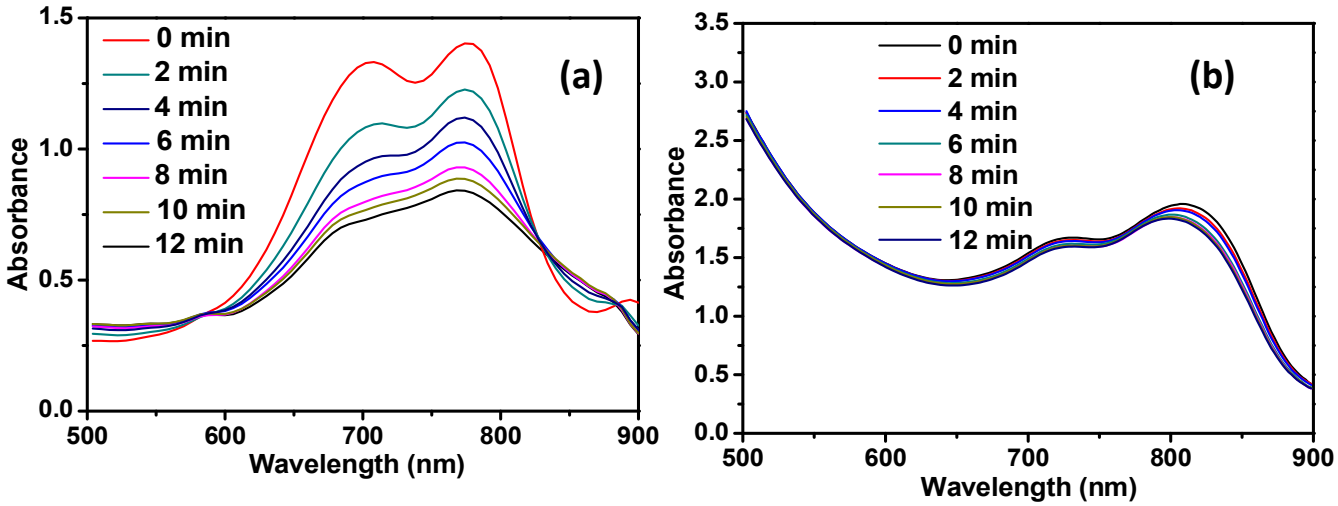

Fig. S15 UV-vis-NIR absorption spectra of (a) free ICG and (b) FPINs aqueous solution irradiated with an 808 nm laser for different times. The initial ICG concentration is 20 μg/mL.

Table S2 Comparison of different photothermal agents.

Materials	Content (μg/mL)	Laser density (W/cm^2)	Time (s)	Wavelength (nm)	η (%)	Ref
FPINs	125	0.88	300	808	25.3	This work
AuNRs@ZIF-8	-	2	600	808	22.7	S1
UiO-66@PAN	100	1.5	300	808	21.6	S2
BSA/SAs–NMOF	200	1	600	660	40.53	S3
PDA-PCM@ ZIF-8/DOX	100	1.5	300	808	30.61	S4
Cy@ZIF-8	20	0.8	300	808	33.2	S5
MCP NPs	50	1	900	808	41.3	S6
siRNA/Zr-FeP	50	1.9	600	635	33.7	S7
UiO-66@CyP	25	1	300	808	27.3	S8
NMOF-SNO	600	1	600	808	48.3	S9

S1 L. Fang, W. Wang, Y. Liu, Z. Xie and L. Chen, *Dalton Trans.,* 2017, **46**, 8933.

S2 W. Wang, L. Wang, Y. Li, S. Liu, Z. Xie and X. Jing, *Adv. Mater.*, 2016, **28**, 9320.

S3 W. Zhu, Y. Liu, Z. Yang, L. Zhang, L. Xiao, P. Liu, J. Wang, C. Yi, Z. Xu and J. Ren, *J. Mater. Chem. B*, 2018, **6**, 265-276.

S4 Q. Wu, M. Niu, X. Chen, L. Tan, C. Fu, X. Ren, J. Ren, L. Li, K. Xu, H. Zhong and X. Meng, *Biomaterials*, 2018, **162**, 132.

S5 Y. Li, N. Xu, J. Zhou, W. Zhu, L. Li, M. Dong, H. Yu, L. Wang, W. Liu and Z. Xie, *Biomater. Sci.*, 2018, DOI: 10.1039/C8BM00830B.

S6 D. Wang, H. Wu, J. Zhou, P. Xu, C. Wang, R. Shi, H. Wang, H. Wang, Z. Guo and Q. Chen, *Adv. Sci.*, 2018, **5**, 1800287.

S7 K. Zhang, X. Meng, Y. Cao, Z. Yang, H. Dong, Y. Zhang, H. Lu, Z. Shi and X. Zhang, *Adv. Funct. Mater.,* 2018, 1804634.

S8 W. Wang, L. Wang, S. Liu and Z. Xie, *Bioconjugate Chem.*, 2017, **28**, 2784.

S9 H. Zhang, X.-T. Tian, Y. Shang, Y.-H. Li and X.-B. Yin, *ACS Appl. Mater. Interfaces*, 2018, **10**, 28390.

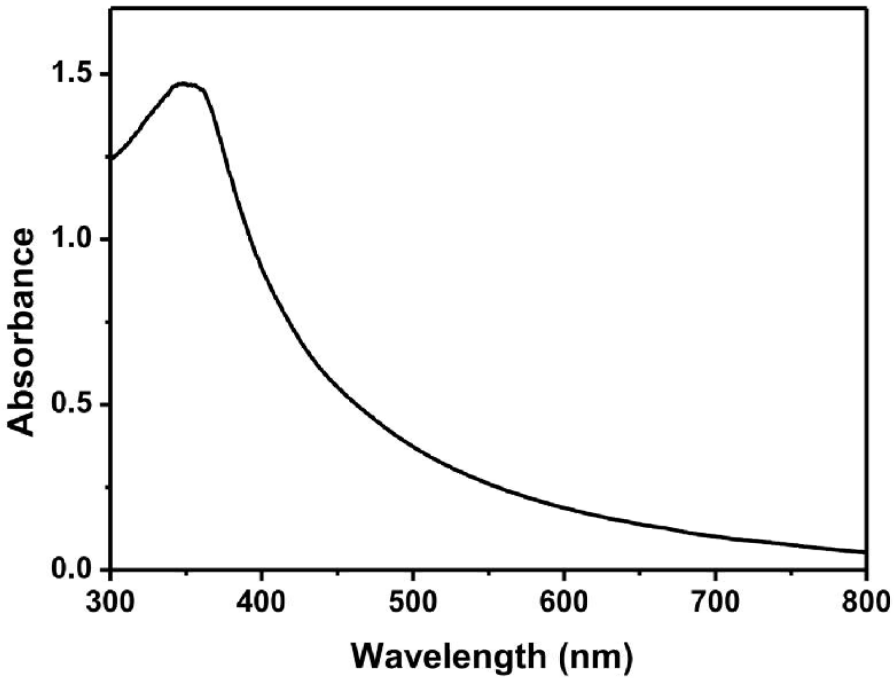

Fig. S16 UV-vis-NIR absorption spectra of Fe-**soc**-MOF@PEG aqueous solution.

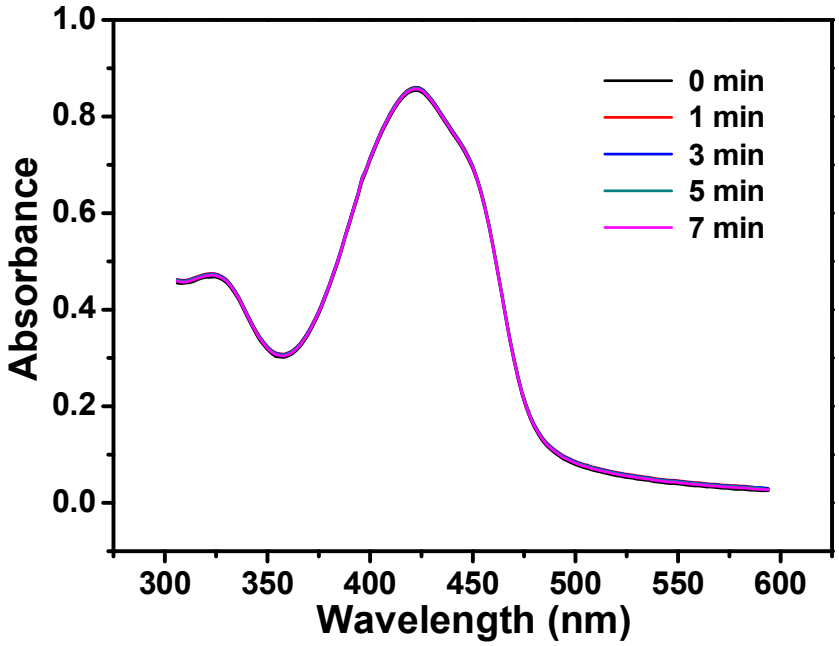

Fig. S17 UV-vis absorption spectra of DPBF solution without FPINs after irradiated under an 808 nm laser for seven minutes.

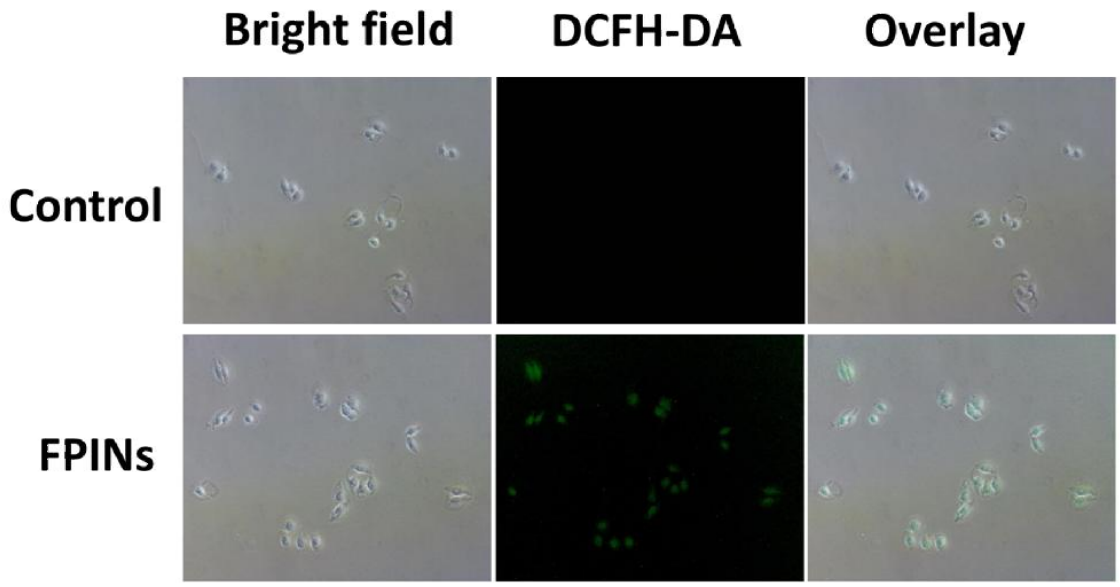

Fig. S18 Generation of ROS in the presence of FPINs in HeLa cells. The upper row shows fluorescent images of the control group. The lower row shows fluorescent images of FPINs-treated cells.

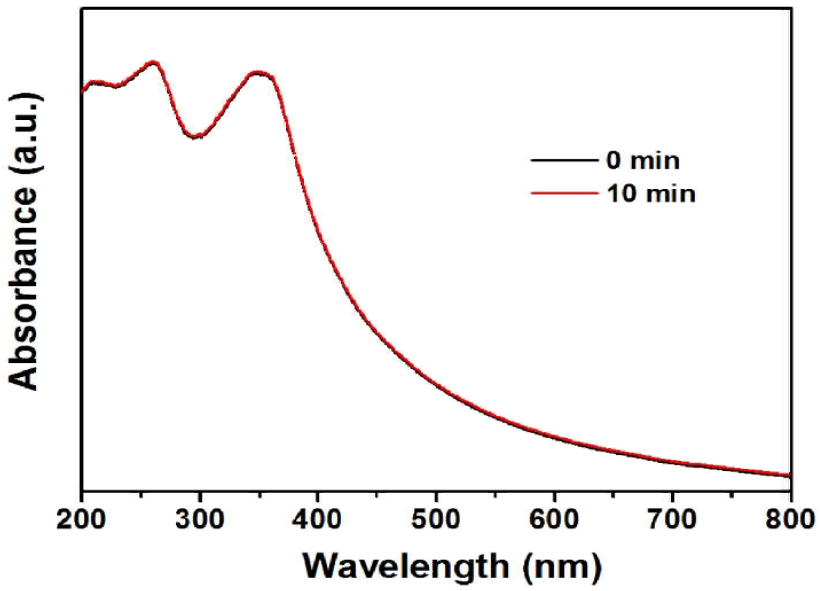

Fig. S19 The UV-vis-NIR absorption spectra of Fe-**soc**-MOF@PEG before and after irradiated by an 808 nm laser for 10 min.

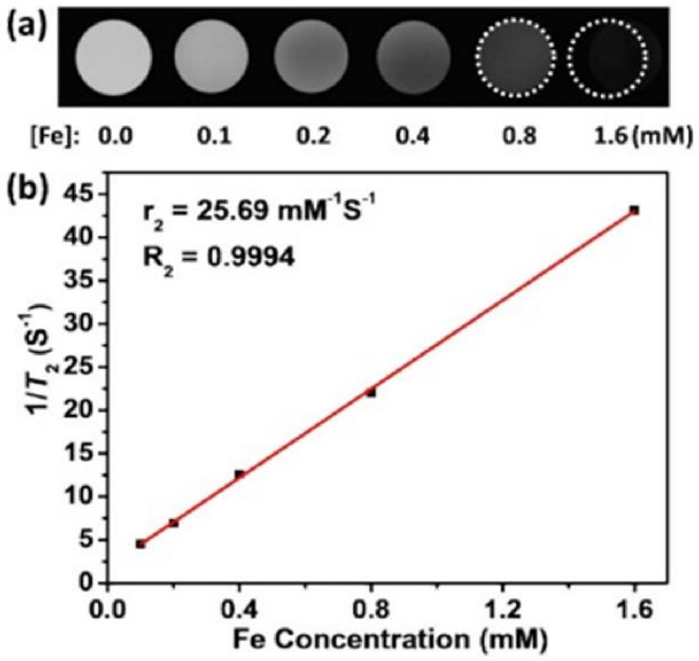

Fig. S20 (a) T_2-weighted MR images of FPINs dispersed in water with different concentrations, and relaxation rate R_2 ($1/T_2$) versus different concentrations of FPINs at room temperature.

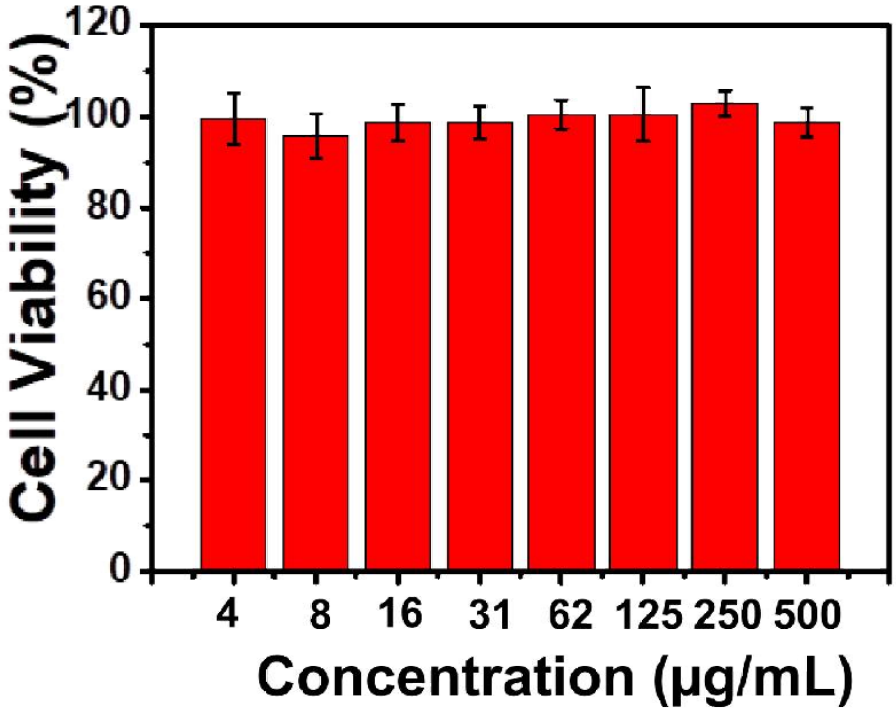

Fig. S21 *In vitro* cell viability data of FPINs against L929 cells after incubation for 24 h.

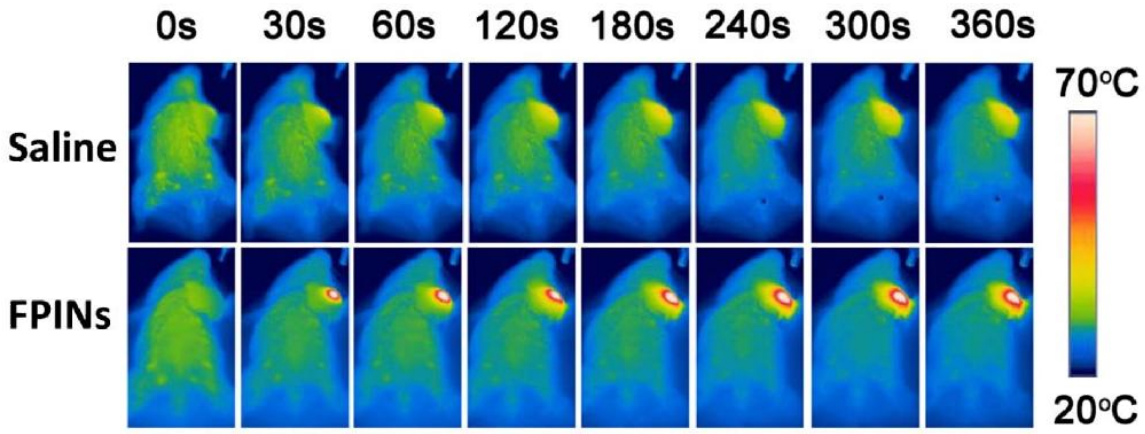

Fig. S22 Infrared thermal images of tumor-bearing mice injected with saline or FPINs solutions after an 808 nm laser irradiation for different times.